Environment Canada
Environnement Canada

The Distribution of Global Radiation over Peyto Glacier, Alberta

Barry Goodison

SCIENTIFIC SERIES NO. 22

INLAND WATERS DIRECTORATE,
WATER RESOURCES BRANCH,
OTTAWA, CANADA, 1972.

Environment Canada
Environnement Canada

The Distribution of Global Radiation over Peyto Glacier, Alberta

Barry Goodison

SCIENTIFIC SERIES NO. 22

INLAND WATERS DIRECTORATE,
WATER RESOURCES BRANCH,
OTTAWA, CANADA, 1972.

Contents

Illustrations

Illustrations (cont'd)

Tables

This study by B. Goodison was undertaken in the summer of 1969. It is one of a series to analyse data obtained during glaciological studies at Peyto glacier, a research basin included in the Canadian contribution to the International Hydrological Decade.

The Distribution of Global Radiation over Peyto Glacier, Alberta

Barry Goodison

INTRODUCTION

Peyto Glacier (50° 40'N; 116° 34'W) is an International Hydrological Decade "Representative Basin" being studied by the Glaciology Division, Inland Waters Directorate. Continuous research on the glacier has been carried out each year since 1965; during this period mass balance (accumulation and ablation), meteorological, and hydrological data have been collected. In 1969, a detailed study into melt processes on the glacier was initiated. To this end, a micrometeorological site was established on the glacier; continuous measurement of the shortwave components of the radiation balance formed an integral part of this project. This paper presents a method of determining the distribution of global radiation over Peyto Glacier, and shows its relationship to glacier melt.

Physical Setting

Peyto Basin is located in the Waputik Mountains, part of the Canadian Rocky Mountains. The basin has an area of 22.07 km^2 above the stream gauge; 13.72 km^2 (62.2%) is ice. The range in elevation is from 2,000 m to 3,300 m a.s.l.; its predominant aspect is northeast (Fig. 1). The basin boundary coincides with two major divides. On the west, the peaks and ridges (e.g., Mount Baker, Trapper Peak) form part of the continental divide, whilst to the southeast Mount Thompson and Portal Peak form part of the divide of the north and south basins of the Saskatchewan River.

The glacier is divided into two distinct physical sections by a 100-m high icefall at the 2,400-m level. Below this, the tongue of the glacier descends 2.4 km down Peyto Valley; this portion is only 16.5% of the total glacier area (Sedgwick, 1966, p. 18). Four distinct lobes make up the area above the icefall; they are the northwestern, western, southern, and central sections (Fig. 1). The different slopes and aspects of these basins have in turn a definite effect on the distribution of radiation over the basin and theoretically on the distribution of melt.

DETERMINATION OF GLOBAL RADIATION

Global radiation (Q_S) is defined as the downward direct (I_d) and diffuse (D) solar radiation as recorded on a horizontal surface from a solid angle of 2π (Canada, Department of Transport, p. iii). The global radiation received on a horizontal surface per day can be expressed as:

$$Q_s = I_d + D$$

A theoretical determination of Q_S involves the assimilation of several independent variables, including declination of the sun, latitude, optical air mass and dust attenuation. The first step in any calculation is the determination or estimation of the extra-terrestrial solar radiation per day on a horizontal plane, and then the adjustment of this value for atmospheric transmission and attenuation by pollutants in some form or other (Bolsenga, 1964). Theoretical calculations of global radiation on and at the ground can be performed for cloudless days, but continual cloudfree periods are rare. Thus, to obtain day-to-day radiation totals during all types of weather conditions, continuous measurement of radiation at a site is necessary.

The immediate problem, however, for Peyto Glacier was the determination of the distribution of global radiation over the basin, adjusting measured values at a point for specific aspects and gradients. To solve this problem, the approach of Atsumu Ohmura (McGill University) was adopted.

Ohmura's method calculates global radiation at a number of points in a basin, allowing for the declination of the sun, latitude of the site, time, and azimuth and gradient of the slope at each point. Ohmura (1968), Garnier (1968), and Garnier and Ohmura (1968;1970) summarize Ohmura's work and procedure for calculating global radiation on slopes.

It is not deemed necessary to repeat the method or equations here as Garnier and Ohmura (1968) give a good explanation of the technique. Sellers' (1965) and List's (1966) approaches, however, are useful aids in following the discussion. A key feature of the approach, which must not be neglected, is that actual radiation values are required in order to determine the atmospheric transmissivity for the time period under consideration. Although for completely cloudless days it is possible to obtain good approximations of this value by standard graphs (e.g., Bolsenga, 1964, p.4) this was not deemed necessary for the study on Peyto Glacier. Instead the measured direct radiation was compared with the calculated extraterrestrial radiation in order to determine the atmospheric transmissivity for that time period.

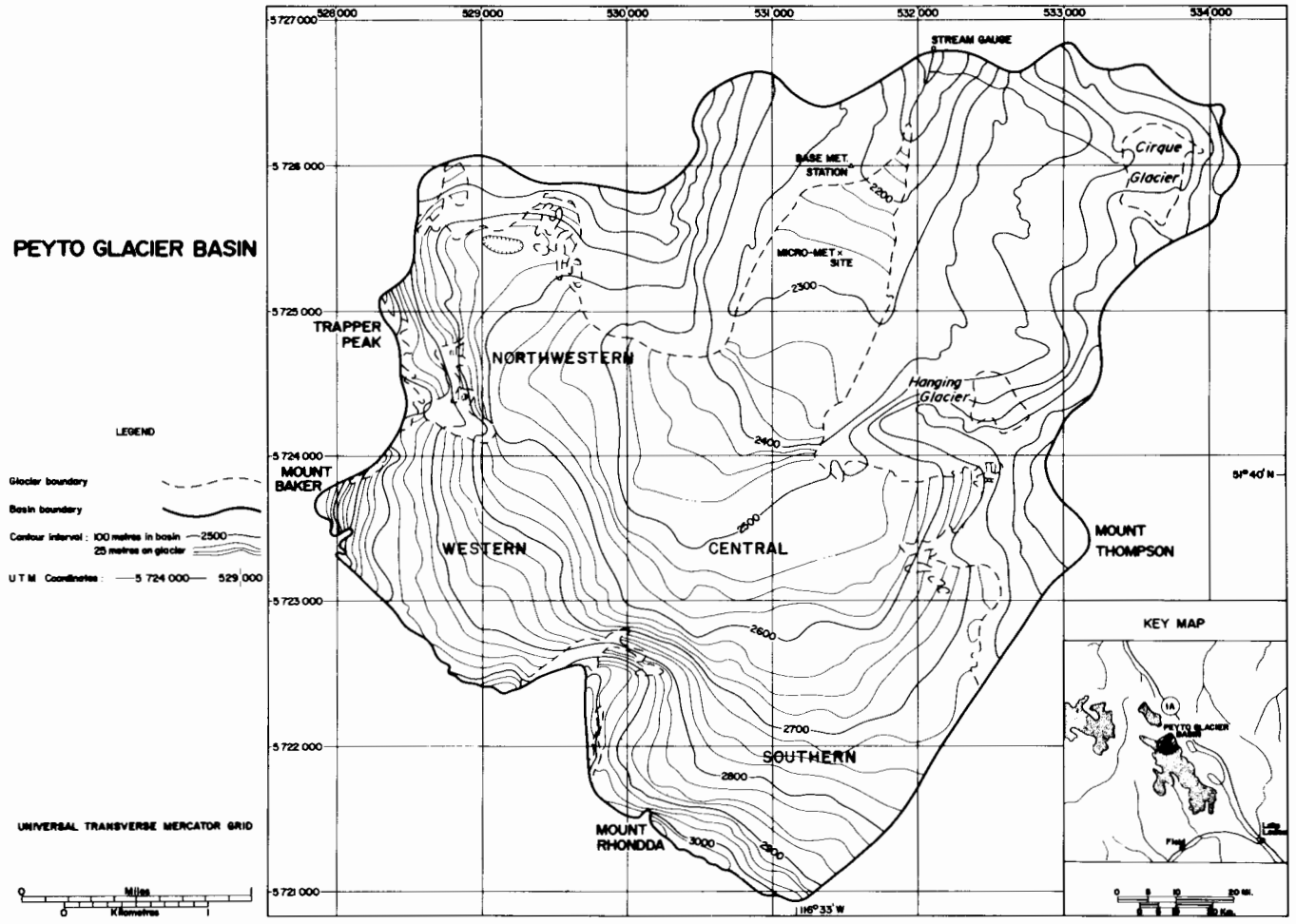

Figure 1. Peyto Glacier Basin.

To facilitate computational procedure, a computer program written by Ohmura was used to print out a map portraying basin variations of direct solar radiation. The original program was modified by Ohmura to include the contribution of diffuse sky radiation. To adjust the diffuse value for various slopes Kondrat'yev's (1965, p.332) formula was used. Simply, it states that:

$$D_S = D \cos^2 \frac{a}{2}$$

where: D_S is the flux of diffuse solar radiation on the surface of the slope,
D is the flux of the scattered radiation for a horizontal surface,
a is the angle of the slope.

The assumptions involved are that the diffuse radiation falling on the horizontal surface is isotropic, and that the temperature and optical properties of the slope and adjoining horizontal surfaces are the same.

Subsequent modifications of the program have been made by the author. Besides the map of global radiation, the actual values calculated for the selected basin points can be printed in matrix form. The program allows also for repeated calculations which may involve data from more than one basin or for different time periods throughout the year for the same basin. Finally, the author has included an option for adjusting the hour angle at each point. This, in effect, adjusts the calculated radiation at each point for shadow caused by the surrounding relief. The shadow effect will be discussed more fully later.

PROCEDURE FOR PEYTO GLACIER

Instrumentation and Available Data

Prior to and including 1969, the total daily incident shortwave radiation (direct and diffuse) was measured at a site near the glacier tongue with a horizontally-installed pyranometer. These measurements are of limited value in this study as the individual components are unknown.

Figure 2. Kipp and Zonen pyranometers used to measure global and reflected radiation over Peyto Glacier.

Figure 3. Kipp and Zonen pyranometer measuring diffuse radiation only.

In June 1969, two Kipp and Zonen pyranometers were installed at a micrometeorological site located on the tongue of the glacier (Fig. 1). Mounted on a dexion frame, the instruments were designed to measure reflected, and direct and diffuse shortwave radiation. Figure 2 shows the instruments set up to measure reflected radiation from the ice, and incoming direct and diffuse radiation.

For this particular study, however, it was necessary to separate direct and diffuse radiation. To achieve this, an adjustable shading ring was constructed and attached to one of the Kipp and Zonen instruments. For diffuse readings, the ring could be set in the desired position, so that the entire glass bulb of the pyranometer was shaded to prevent errors from multiple reflections at the glass surface (Fig. 3).

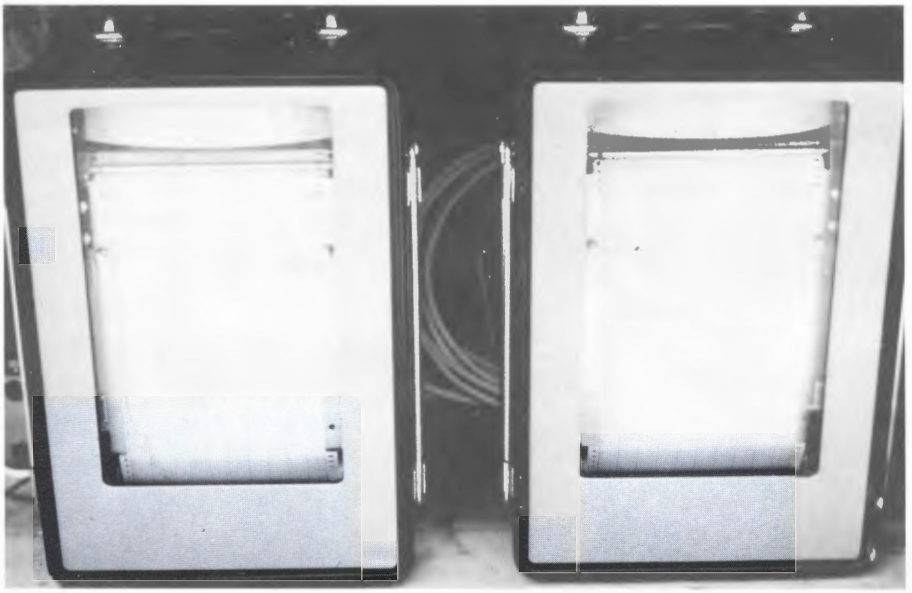

Figure 4. Recorders providing continuous record of reflected (left) and global (right) radiation.

Since a correction factor to allow for the diffuse radiation intercepted by the ring was not determined, the shading disc on the ring was kept as narrow as possible in order to keep the error small. Because of this, the disc had to be moved along the ring several times during the day to provide continuous shade for the glass bulb. In operation this was not a serious problem since the micrometeorological site received constant attention. Other readings were made every two hours at the site and many of the instruments needed re-levelling because of irregular ice melt; the latter problem was of particular concern in the measurement of radiation.

When diffuse radiation was recorded continuously during the day, the second pyranometer was used for measuring direct plus diffuse radiation. By subtraction of the measured daily totals of each component, direct and diffuse shortwave radiation inputs could be determined. There was no problem in comparing values obtained from each instrument since they were both calibrated by the Department of Transport (now Atmospheric Environment Service).

If only one instrument is available for computing direct and diffuse radiation, then shading of the instrument for short intervals throughout the day could provide an alternative method of estimating each component. Since a continuous trace of the radiation fluctuations is provided on the recorder (Fig. 4) interpolation between samples would not be too difficult. Success with this method, however, is limited generally to cloudless days.

The most serious measurement problem was caused by shadow from surrounding peaks; for example, on July 1 the micrometeorological site receives direct shortwave radiation for only 75% of the possible maximum number of hours. The hours of shadow are early in the morning and late in the evening. A problem arises in trying to apply these measured values to the upper part of the basin where losses due to shadow are much less. Adjustments made for this factor will be discussed later; however, it is realized this problem could be overcome by installation of similar recorders in the upper part of the basin, perhaps on a small rock outcrop in the centre basin. If it were installed on land, and an adequate shading ring attached, then the instruments would not need continuous care and the data would be of greater use in the study of radiation distribution over the glacier.

Sun-Path Diagrams and Horizon Determination

In order to determine accurately the number of hours of sunshine at various locations over the glacier, it was necessary to construct a sun-path diagram for Peyto (Fig. 5) and to superimpose on the diagram the local horizon at different locations.

The sun-path diagram was constructed from Azimuth and Altitude Tables published by the U.S. Navy, Hydrographic Office (1940). Azimuth is plotted from north through east on a circular net, while the altitude is plotted 0° to 90° from the outside of the circle to the centre (Fig. 5). Similar diagrams for other latitudes may be found in List (1966). For this project the sun's path was plotted only for 0° to $+23.5^\circ$ declination (March 21 to September 23, inclusive). This period adequately covers the time when ripening of the snowpack and subsequent snowmelt affect Peyto Glacier.

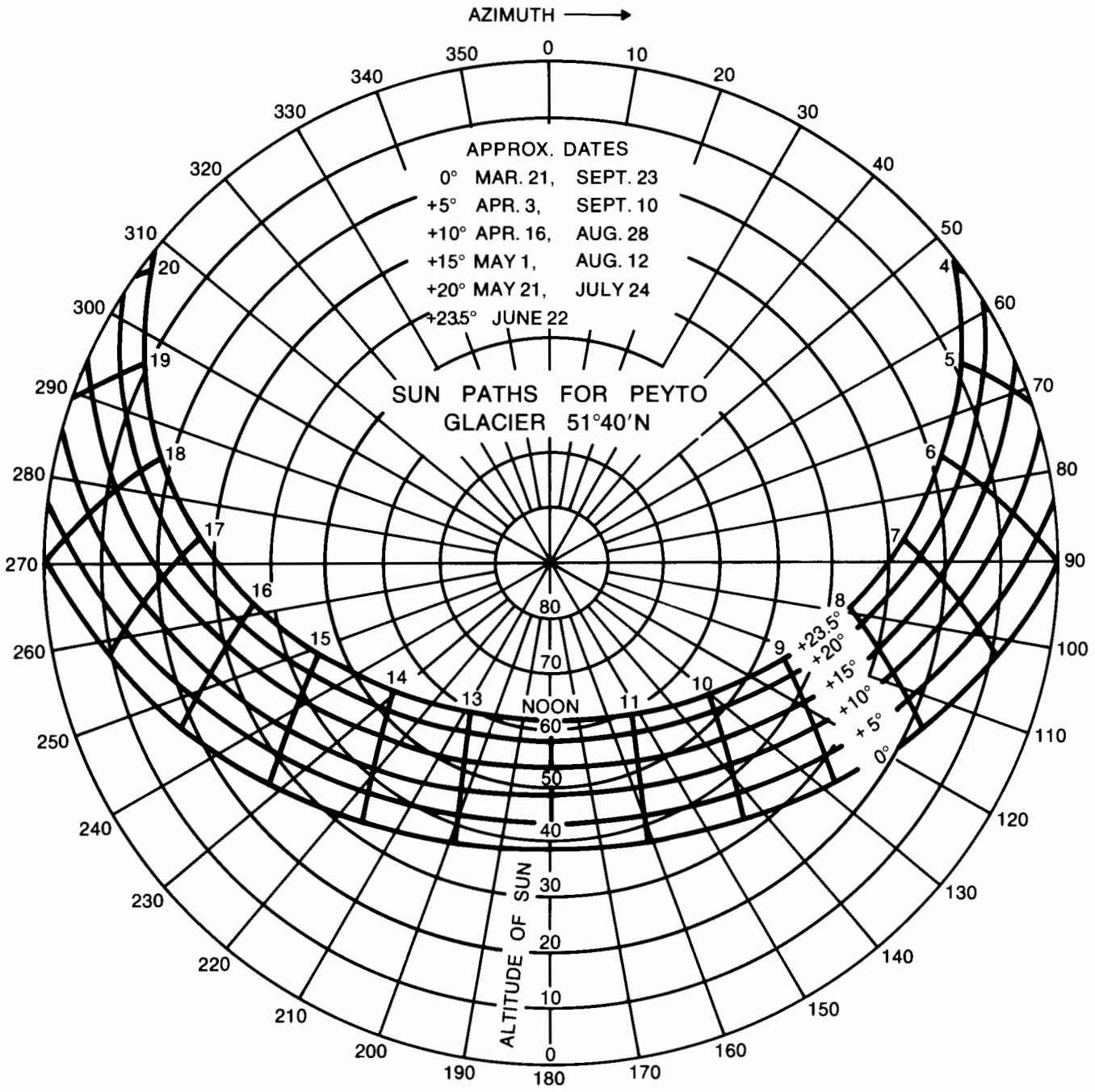

Figure 5. Sun-path diagram for Peyto Glacier.

To determine the amount of sunshine incident on any location on the glacier, the local horizon for that point is plotted on the sun-path diagram. Figure 6 shows the horizon at the micrometeorological site, while Figure 7 provides the same information for the base camp meteorological site. Both of these horizons were determined accurately by theodolite. To measure the horizon at numerous points on the glacier by theodolite would be ideal, but because of the difficulty of locating accurately any predetermined point on the glacier, it was necessary to determine the horizon using the 1:10,000 topographic map of Peyto Glacier. The accuracy tends to be reduced, but comparison of the two methods at the micrometeorological site indicated about a 3% – 5% difference in the determination of the angle of the horizon. This is a negligible error when one considers the scale at which the sun-path

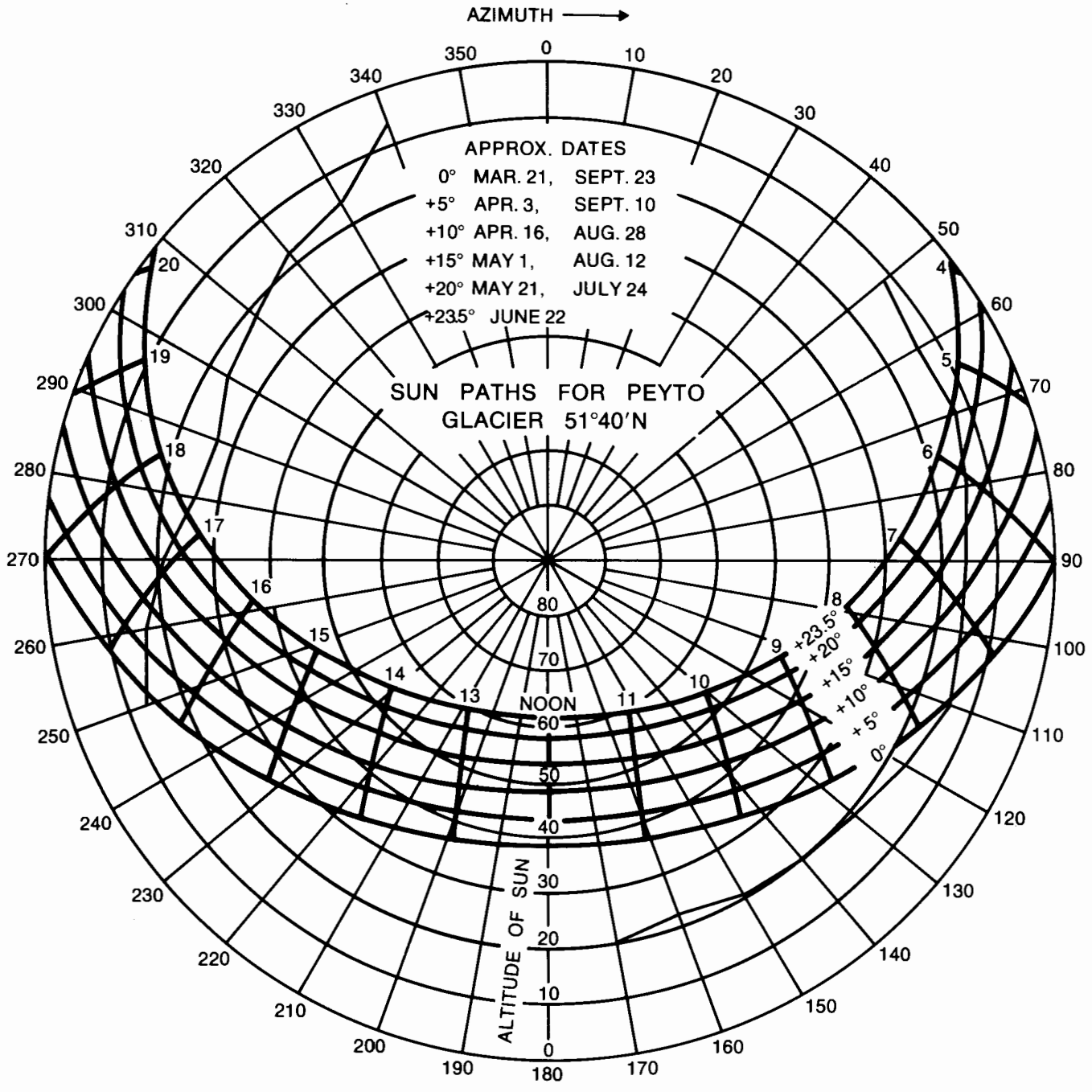

Figure 6. Horizon at micrometeorological site.

diagrams are constructed. To help determine the horizon from the map, the prominent points on the horizon were checked in the field and located accurately on the map. The greatest error in the horizon diagram results from its construction at approximately 10° intervals and the necessity of having straight line interpolation between points. The magnitude of the error involved would vary for every location, but since higher relief points were used on the topographic map, the results would tend to reduce the number of hours of sunshine at any point for any given time.

Comparison of the number of hours of sunshine at the base meteorological site as determined by this method and by measurement with a sunshine recorder showed no difference in the time the sun first shines and last shines on

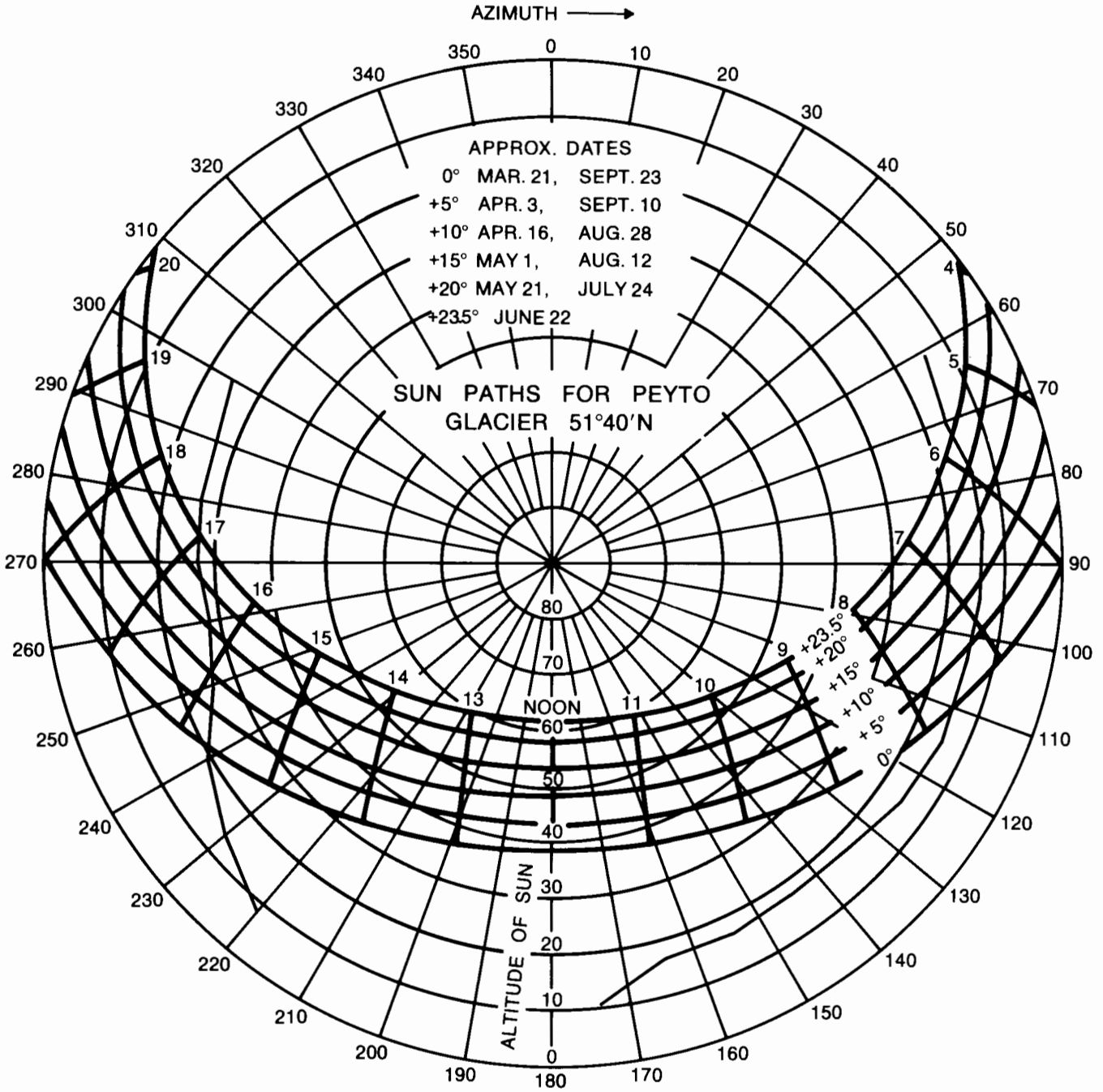

Figure 7. Horizon for base-camp site.

the site. This confirms that the horizon diagrams are as accurate as possible.

Using the Universal Transverse Mercator (UTM) Co-ordinate System as a reference for location of points, horizon diagrams were constructed for several selected sites on the glacier. The tongue of the glacier was covered in greatest detail because it is the area most affected by shadow. In the upper basins, a representative coverage of the area was obtained using a small number of carefully-selected points.

All of these diagrams were used in the calculation of the shadow effect over the basin. For any chosen day, it is possible to determine from the diagrams the time when the sun first shines and last shines on any of the selected

locations. The intersection of the horizon with the sun-path for the day under study gives this information. In this study July 1 and August 16 to September 1 were the periods studied.

For the selected points, the necessary morning and evening hours angles are obtained; by interpolation, the hour angles at the other glacier locations are determined. The effect of the surrounding terrain is readily seen from these values. In the morning the sun strikes the western and southwestern parts of the upper basins earliest; the tongue of the glacier shows the same pattern, but later in the day than the upper part of the basin. In the evening, as expected, the sun leaves the western (i.e., east-facing slopes) basin first; a later hour of sunset is experienced at the eastern points in the basin. The tongue, as in the morning, has shadow over it while the upper basins have sunshine. Because of the location of the mountains on either side of the glacier tongue, the movement of shadow across the ice is not the same in the morning as in the evening. The close proximity of Peyto Peak to the ice results in an early shadow in the evening.

The upper basin does not receive as many more hours of sunshine as one might first expect. It is noted that usually those points that have a comparatively early sunrise, have an early sunset, or vice versa. However, the upper-basin locations do have more hours of sunshine compared to points on the tongue, but since this extra time occurs when the sun is at a low angle, the total energy input is not much more than that at the micrometeorological site. As the declination of the sun decreases in late August and early September, the absolute number of sunshine hours on any day decreases at rates which depend upon the location of the surrounding mountains. For many points on the edge of the glacier below the icefall, shadow becomes very pronounced. However, in general, the relative shadow effect during high sun periods (June-July) compared to lower sun periods (August-September) is almost the same; that is, the percentage of total possible sunshine hours lost because of shadow is about the same. By late September, however, shadow becomes more prominent, but by this time ablation is low. The differences resulting from the inclusion of shadow in the analysis, and the effect it has on ablation will be shown in the discussion of the results.

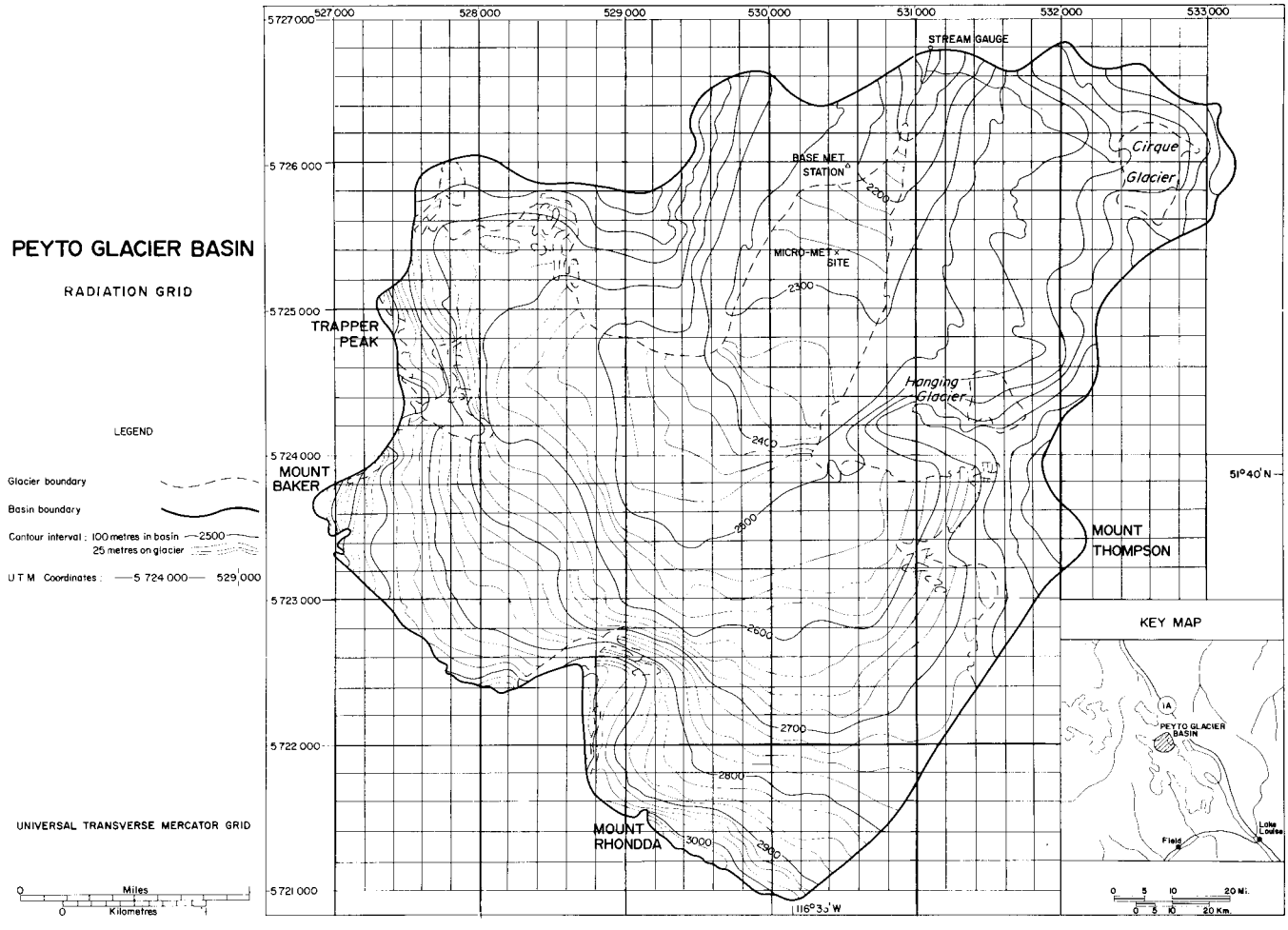

Figure 8. Peyto Glacier Basin radiation grid.

It should be emphasized that the radiation instruments were located in one of the areas where shadow had a significant effect and where the hours of sunshine were lowest. This makes it difficult to use the measured radiation totals and to apply the same absolute values, particularly the diffuse value, to other parts of the basin which receive more hours of sunshine.

The Determination of Azimuth and Gradient

Following the UTM system, a regular 200-m grid was established over the glacier and basin area. For each point in the glacier basin it was necessary to determine the azimuth and gradient from the 1:10,000 topographic map; this is a major manual task. The grid established over the basin is shown in Figure 8. The smaller scale map, instead of the 1:10,000 map, is used here for convenience. The selection of the grid interval was subjective, but since there are no great topographic irregularities on the glacier itself, it is felt that the points are close enough.

To determine the azimuth at each point, a circular grid representing the compass directions (Fig. 9) is required, the size of the grid varying with the size of the basin and the scale of the map. All that is involved is the establishment of a net spaced at 10° intervals and measured positively north through east. Outward from the centre are circles whose diameters represent selected horizontal distances on the ground; these are used for calculating the gradient at each point. By placing the centre of the net over an intersection point, and orientating it towards true north (i.e., 0° 21'W of UTM grid north), one may obtain the azimuth by determining the mean downslope direction for that point. This is recorded to the nearest 10 degrees.

At the same time the difference in elevation over a selected horizontal distance (say 100 – 200 m, depending on the irregularity of the slope) can be obtained by counting the number of contours within the 100 or 200 m diameter circle. Using these values and referring to Figure 10, one can obtain the appropriate gradient for the intersection point. This procedure of determining the azimuth and gradient is then repeated for all points within the basin. One comment worthy of repetition is that azimuth and gradient values refer to a "meso-slope" for the point rather than the "micro-slope". Since the measurements were obtained from the topographic map, they cannot represent the micro aspects surrounding a specific point. As the ice is exposed, it becomes very hummocky and irregular (Figs. 2 and 3). The topographic map provides a meso- and macro-slope, while field observation shows that any given point on the ice may have an entirely different aspect and gradient because of the very irregular surfaces not recorded on the map. This problem cannot be overcome, and one must keep in mind that this difference exists.

The Determination of the Hour Angles

For the days selected, it is necessary to obtain from the Smithsonian Meteorological Tables (List, 1966) the declination of the sun (this is independent of latitude) and the appropriate hour angles, corresponding to when the sun first shines and last shines on the slope. These latter two values vary not only daily, but also according to latitude. If there is no shadow on the site from the surrounding terrain, then the hour angles would correspond to the times of sunrise and sunset. The hour angle is zero at solar noon, that is when the sun is directly south of the observation point, and increases by 15° for every hour before or after solar noon. At 0630, for example, the hour angle is −82.5° or −1.440 radians.

For Peyto Glacier, shadow is dominant so the hour angle is calculated for the intersection of the horizon and sun-path. For July 1 the hour angles are −1.720 and +1.382 radians, corresponding to the solar time when the sun first shines and last shines on the instrument site; for September 1, they are −1.306 and +1.267 respectively.

In considering shadow throughout the basin the hour angles (in radians) were determined for the selected sites on the glacier for which horizon diagrams were previously constructed. Interpolation of values for points between these sites is then possible. Unfortunately, this is a time-consuming procedure, and since the hour angle varies almost daily, the recomputation for every day or at least every other day, when studying a long time period, will involve considerable time. This is not a serious problem around the time of the solstice, since the declination of the sun changes very little and the hour angles will be approximately the same for several days. The problem is more serious through the equinox period, since the declination changes rapidly with time. Once the hour angles are determined for different days, however, they will apply for every year and will not have to be recalculated. In the meantime, this is a manual task which is necessary in the consideration of shadow over Peyto Glacier. It should be noted that horizon diagrams, and therefore the shadow effect, have been completed only for the glacier, and not for points in the non-glacierized parts of the basin. However, data are available for determining the radiation distribution in the basin, excluding the influence of shadow.

The Computer Program – A Technical Description

To cover only the glacier, a grid comprised of 28 rows and 23 columns was used. The computer program is set up to cover only 14 columns when printing out the map. To overcome this problem, the extra columns are added to the bottom of the printout which can subsequently be cut and the data placed in their correct relative positions. The length of the map, designated as L, thus becomes 56 (double the original); if there were 42 columns instead of 23, then the map would be three times longer for the purpose of printing out. The map is printed out with the actual intersection points one inch apart; the program provides a linear interpolation of radiation values between these points.

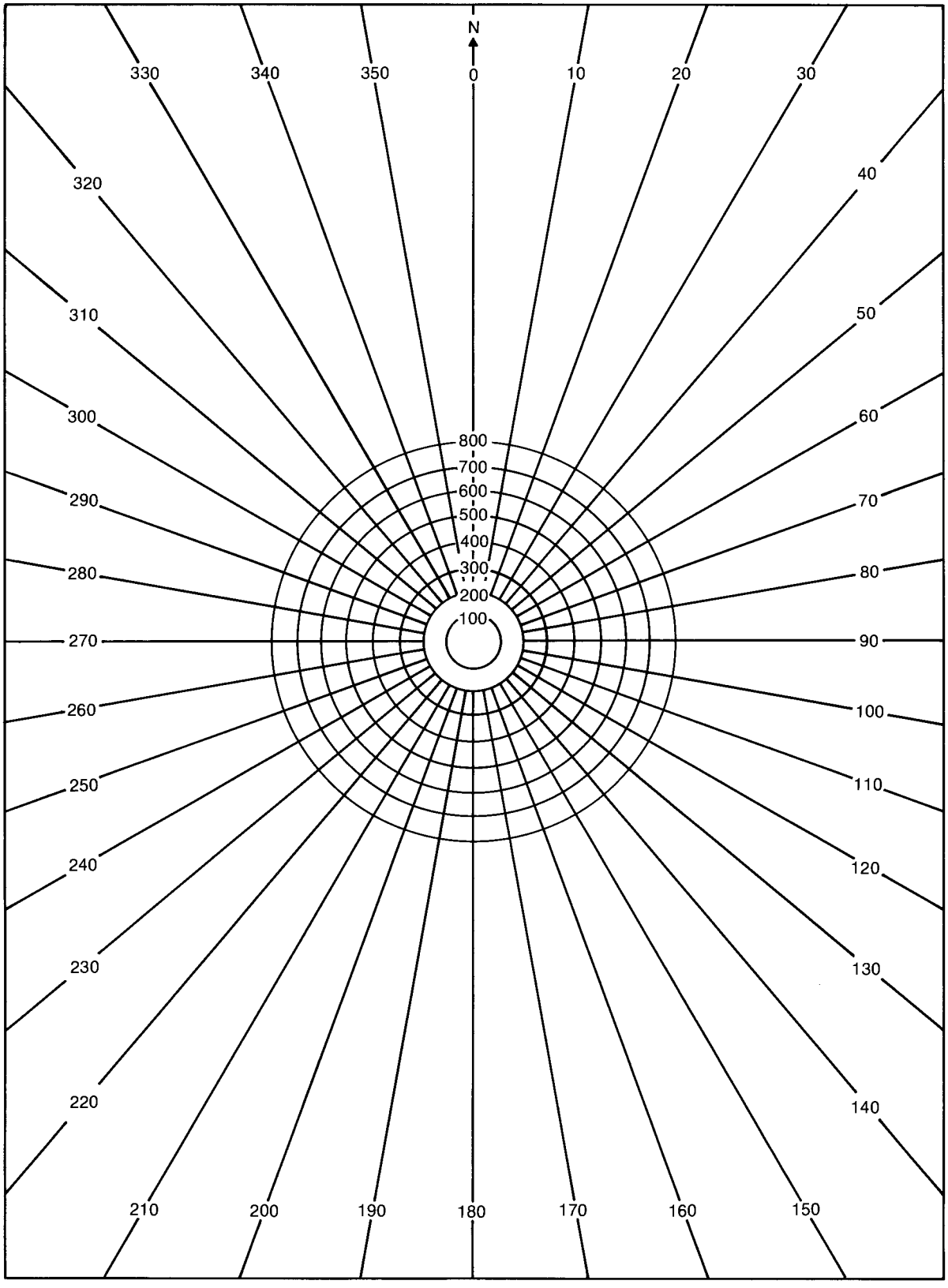

Figure 9. Circular grid for determining azimuth and gradient.

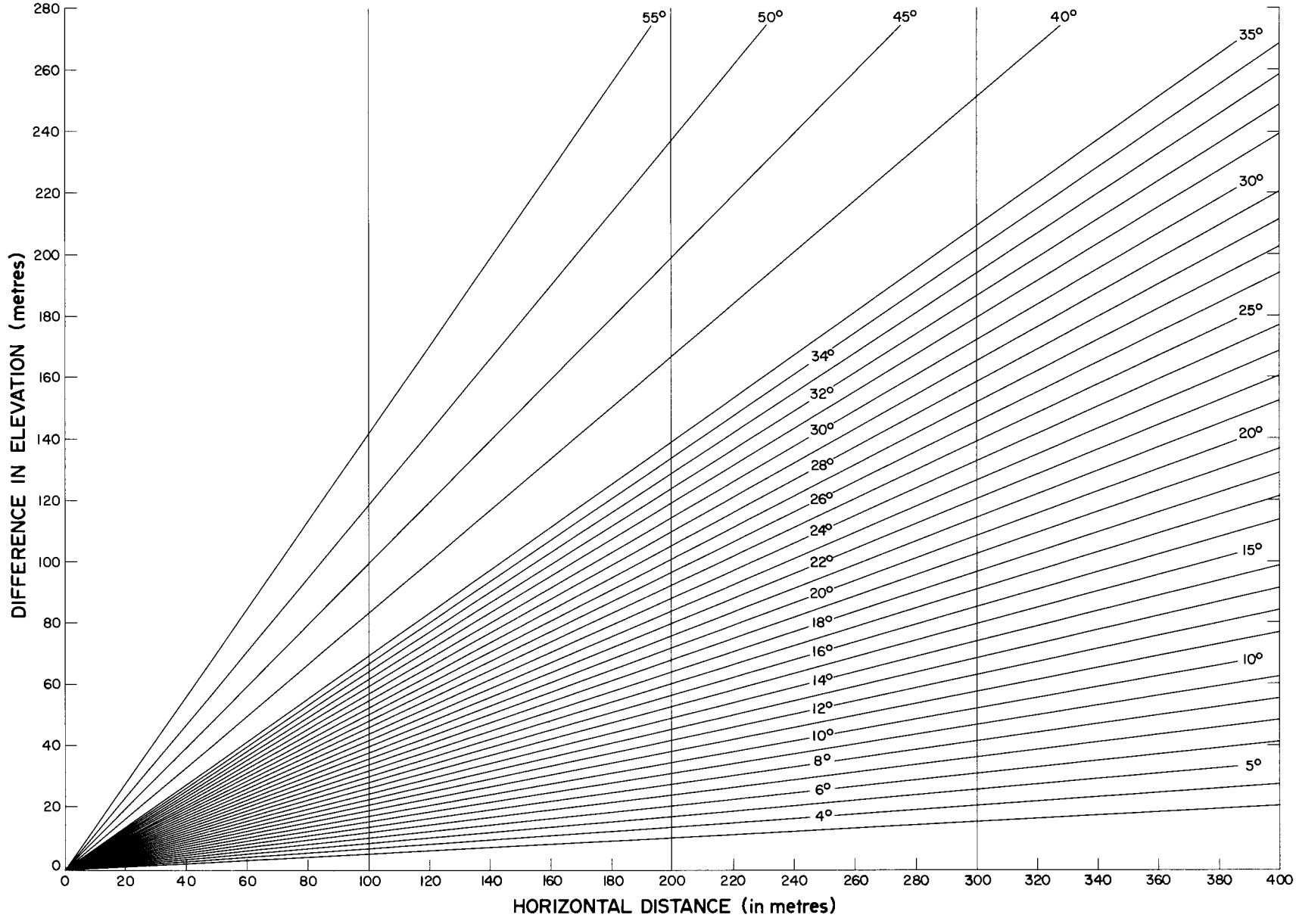

Figure 10. Arc tangent curves.

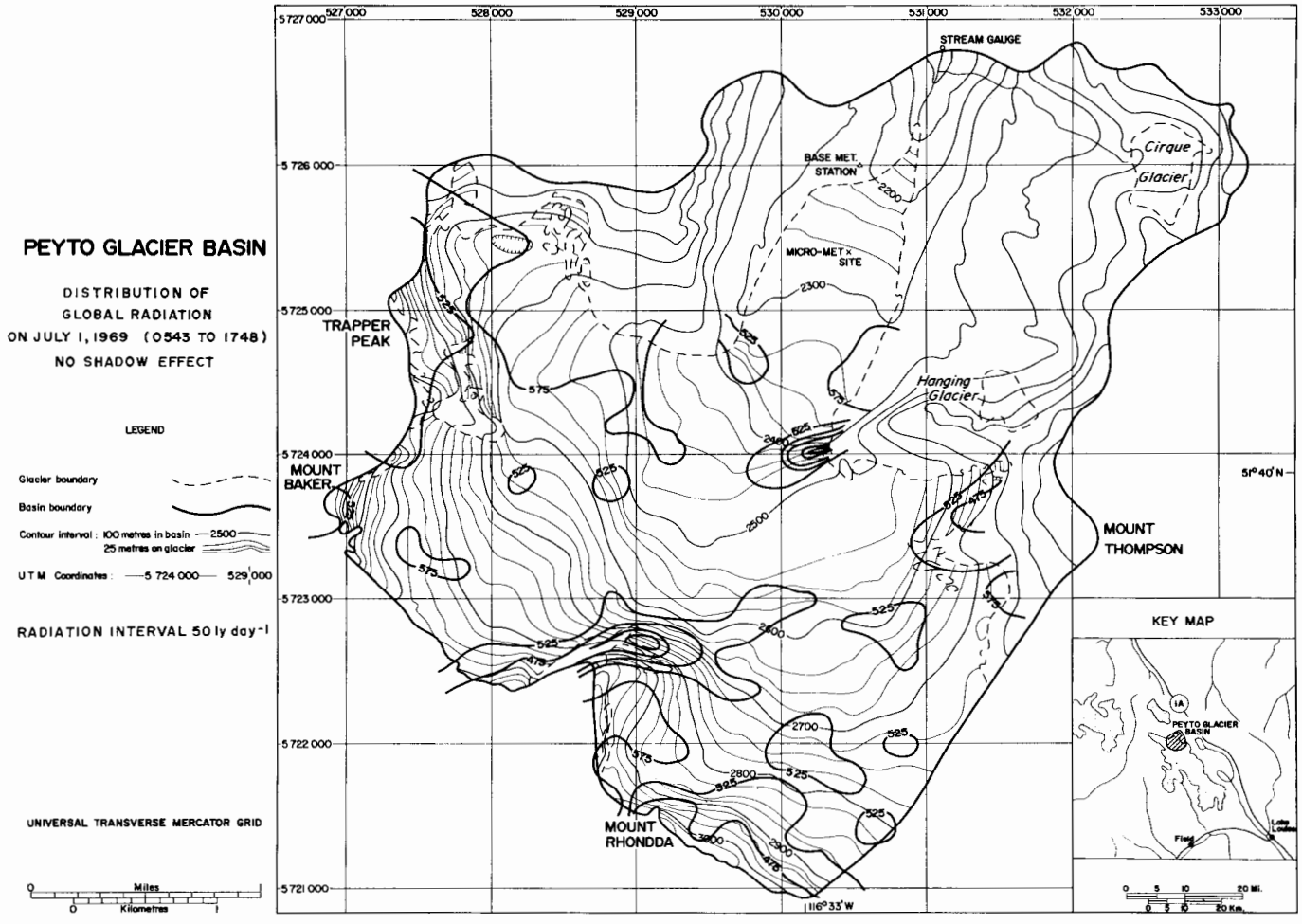

Figure 11. Peyto Glacier Basin, distribution of global radiation on July 1, 1969 (0526 to 1717), no shadow effect.

The data cards containing the azimuths, gradients, morning hour angles, and evening hour angles are punched according to row, with the 14 values for each row appearing on the same card. If the intersection point falls outside the basin boundary, then the azimuth and hour angles are left blank and the gradient is given the value of 90. Thus four sets of 56 data cards are required for Peyto Glacier. For repeated runs for different time periods, only the two sets with the hour angles have to be changed.

Below is a summary of the order and format of all the data cards required for this study:

1. Card with graphing (plotting) symbols.
2. Latitude of station in radians for Peyto this value is 0.9018.
3. The length of the map (L); L = 056 for Peyto Glacier.
4. Cards listing azimuths — the number of cards equals the number of rows, i.e., the length of the map.
5. Cards listing gradients — the number of cards equals the length of the map.
6. Actual data for the site: (all on one card)
   Date
   Declination of the sun — degrees
   — minutes
   Measured direct insolation
   Measured sky-diffuse insolation
7. The hour angles when the sun first (W) and last (W1) strikes the instrument site for the time period under study.
8. Logical true-false statement allowing for the exclusion or inclusion, respectively, of the shadow analysis.
9. Cards listing the hour angles for every basin point when the sun first strikes the slope.
10. Cards listing the hour angles for every basin point when the sun last shines on the slope.

If the hour angles determined for the instrument apply to the entire basin (i.e., no shadow effect), numbers 9 and 10 are not required, and this part of the program can be skipped. Repeat runs with or without the shadow can be made.

The results of the analysis (i.e., the calculated global radiation for each intersection point) are printed out, both

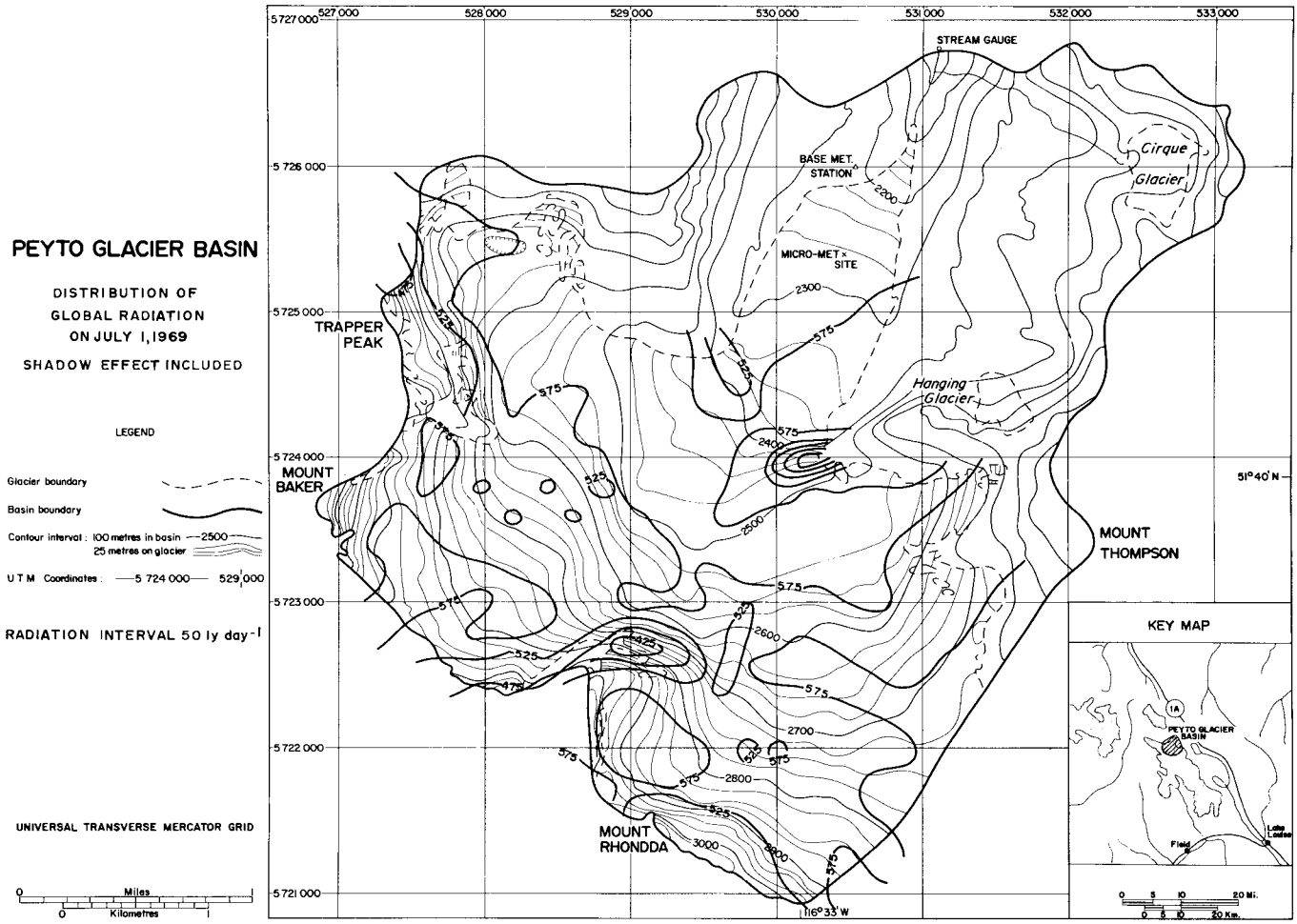

Figure 12. Peyto Glacier Basin, distribution of global radiation on July 1, 1969, shadow effect included.

in matrix and map form. The map is very useful for drawing isolines of radiation, but it is desirable to superimpose these isolines on a contour map such as was done in this study. To facilitate this task the author constructed a grid of 1" squares which had the same pattern of intersection points as the original grid over the basin. The grid can be placed over the computer map to aid in reproducing accurately the isolines on a map of a different scale.

Future computer programming modification may include: a shadow routine based on a "search and find" principle using the heights of the basin perimeter; direct plotting of radiation isolines; and computer computation of azimuths and gradients.

DISTRIBUTION OF GLOBAL RADIATION OVER PEYTO GLACIER

Global radiation data were first collected during the summer of 1969; direct and diffuse totals are available for July 1 and for the period August 16 to September 1. The separation of direct and diffuse radiation was determined for July 1 by intermittently shading the glass bulb with the shading ring. This was satisfactory in the morning when there were no clouds, but clouds in the afternoon limited the accuracy of the separation. For the extended period in late August, continuous daily records for both direct and diffuse radiation were available; however, this meant that no measure of reflected shortwave was possible; consequently, albedo fluctuations could not be analyzed for this period. Table 1, gives the measured radiation data for the micrometeorological site. In the present analysis a solar constant 2.00 ly min^{-1} was used, but comparatives runs were studied using 1.94 ly min^{-1}. As might be expected, the difference in the calculated radiation value for each point was negligible. Although the higher value tends to reduce the transmissivity slightly, the solar constant is in turn used in the equation which calculates the direct radiation for each point. These opposite trends tend to cancel each other out. It was found that for the 17-day period of August 16 – September 1, a solar constant of 2.0 ly min^{-1} gave a calculated 17-day total 11.0 ly (approx. 0.15%) higher than the total obtained by using the 1.94 value; any difference is negligible and all points are equally affected.

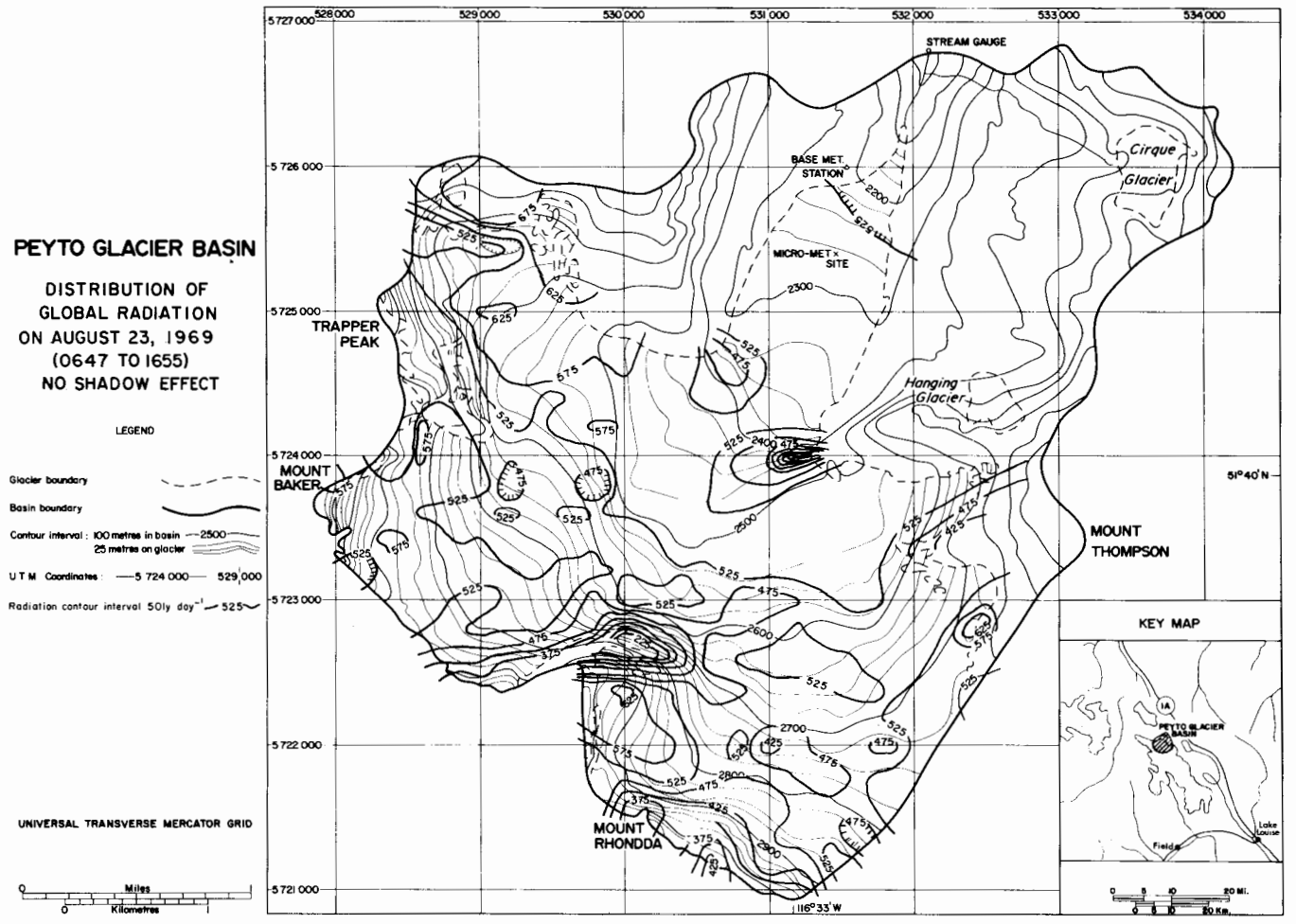

Figure 13. Peyto Glacier Basin, distribution of global radiation on August 23, 1969 (0647–1655), no shadow effect.

Table 1. Summary of radiation measurements

Date	Morning Hour Angle (radians)	Evening Hour Angle (radians)	Direct Insolation (1y day^{-1})	Sky-Diffuse Insolation (1y day^{-1})	Transmissivity
July 1	−1.720	+1.382	440.8	130.7	0.585
Aug. 16	−1.414	+1.311	70.0	240.0	0.200
Aug. 17	−1.407	+1.308	492.0	88.0	0.755
Aug. 18	−1.400	+1.305	206.2	136.0	0.430
Aug. 19	−1.394	+1.302	8.6	130.5	0.050
Aug. 20	−1.389	+1.299	141.0	192.2	0.345
Aug. 21	−1.381	+1.295	43.9	166.2	0.150
Aug. 22	−1.372	+1.292	511.5	69.5	0.800
Aug. 23	−1.365	+1.289	512.7	64.7	0.800
Aug. 24	−1.358	+1.286	397.1	113.4	0.690
Aug. 25	−1.350	+1.283	210.2	164.4	0.465
Aug. 26	−1.343	+1.280	433.1	109.1	0.740
Aug. 27	−1.337	+1.276	102.0	171.9	0.300
Aug. 28	−1.332	+1.274	53.1	257.6	0.200
Aug. 29	−1.326	+1.271	87.1	212.9	0.280
Aug. 30	−1.320	+1.269	63.7	209.9	0.230
Aug. 31	−1.313	+1.268	495.4	83.0	0.830
Sept. 1	−1.306	+1.267	355.0	112.0	0.680

To study adequately the distribution of global radiation, two separate runs for each day were conducted. The first provided a "shadow-free" distribution corresponding to the period of measured global radiation at the micrometeorological site (i.e., the time between the morning and evening hour angles). This is not strictly correct for points on the edge of the glacier very close to the mountains, but since they account for only 2% – 3% of the total glacier area, for comparison purposes it does not affect the analysis. The second run included the effect of shadow over the glacier.

The Kipp and Zonen pyranometer was located in an area of maximum shadow and two assumptions have to be made in the program. First, the transmissivity calculation is based on the direct radiation received at the micrometeorological site and it is assumed that this transmissivity applies over the entire basin. This is not necessarily true, however, since this presumes that conditions over the entire basin are such that a transmissivity of say 0.585 for July 1 applies to periods before 0526 and after 1717. On a clear day this assumption creates no problem, but on days with varying amounts of cloud the transmissivity may be different for these early and late parts of the day. This

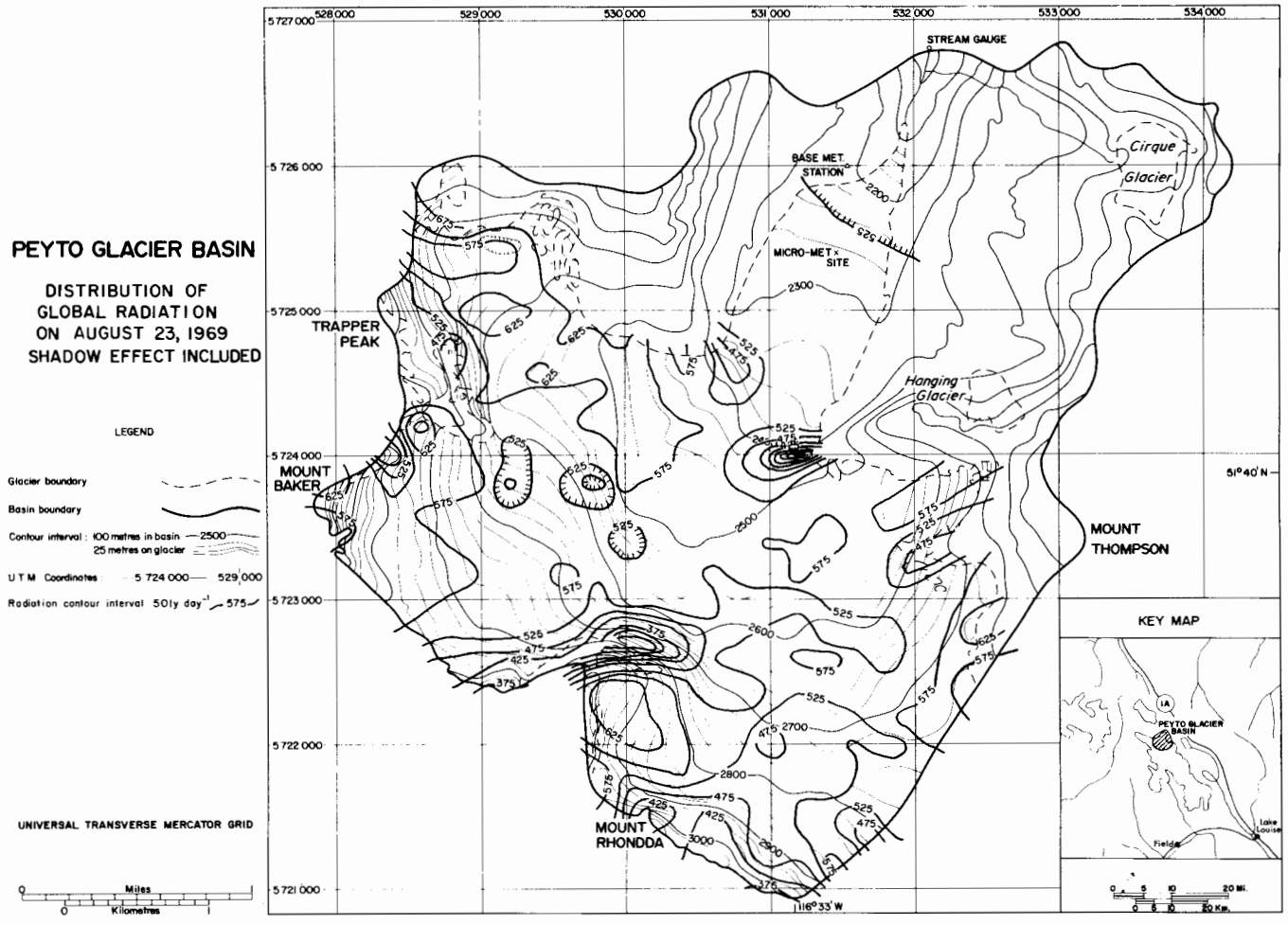

Figure 14. Peyto Glacier Basin, distribution of global radiation on August 23, 1969, shadow effect included.

problem is probably no more serious than having the lower half of the basin clear and the upper part affected by cloud. The calculated transmissivity even for the midday period then would not be applicable over the entire basin. This local drifting of cloud over the upper parts of the basin was observed by the author. In any analysis over an extended period of time, however, this problem would quite probably be self-cancelling.

The second assumption, and perhaps the more serious, is that the absolute diffuse total can be applied to every point in the basin. However, the diffuse value would be higher in areas experiencing a longer period of sunshine or a greater relative cloud cover. Since the absolute direct total is not used in the computation at each point, but instead the relative measure of transmissivity is used, the problem of underestimating the total direct insolation does not arise. Hopefully, the error involved in applying a single transmissivity value over the whole basin is random.

The only way to reduce the error involved is to set up an instrument in the upper basin where shadow is minimal and where recorded values would be more representative of the entire basin.

The results of two runs for July 1 are shown in Figure 11 and Figure 12. Figure 13 and Figure 14 show the distribution for a day later in the summer—August 23. The striking result for both days is that for comparable runs of "shadow" and "no-shadow" the pattern of distribution is similar for each (although the absolute values are different in the two runs); north-facing, steep slopes are notably low, south-, east- and west-facing slopes are high. The pattern differences of July 1 and August 23 are mainly those of extremes, that is, the range of incoming radiation is much greater on August 23 as the lower declination of the sun begins to affect southerly-facing steeper slopes (causing higher values) and north-facing slopes (causing lower values). The July 1 pattern is fairly even. Zones of equal radiation extend along the NW-SE trend of the upper basins, with the absolute range of values being low. This more uniform distribution is caused by the fact that the sun in summer is fairly uniform for both north- and south-facing slopes, and because the relatively low intensities on a gently-tilted north slope are compensated by a longer

potential sunshine duration than that existing on a south slope. Thus, gradient is more influential than azimuth in this high sun period (Ohmura, 1968).

As the declination of the sun decreases, the pattern of August 23 becomes more dominant. The steeper southerly-facing slopes receive more radiation than the gently tilted slopes; north-facing slopes receive even less. There is a much more variable pattern, and although the basic bands of radiation are similar to July 1 the extremes are greater.

For both periods the greatest amount of global radiation is received in the south-southeasterly-sloping northwestern lobe. This area is clearly seen in Figure 15; also shown are the variable slopes and contrasting aspects of the basin which result in the variable radiation distribution over the glacier. For both periods the tongue has a fairly uniform distribution, with differences being accentuated when shadow is considered. However, the least amount of radiation is received on the very steep north-facing slopes, all of which are associated with prominent relief features. The most predominant area in this regard is the icefall where the global radiation is about 40%–50% lower on July 1 and 70%–75% lower on August 23 than the rest of the glacier on the corresponding days. The other low area is in the upper basin northwest of Mt. Rhondda; again on August 23 the percentage decrease here is much greater than the July 1 decrease because of the increased importance of aspect. The shadow present in these steep areas is visible in Figure 16. For both periods these areas with very low values have the same pattern whether or not effective shadow from the surrounding peaks is included.

Comparing Figures 11 and 12 and Figures 13 and 14 for differences because of shadow, one notes that the differences are not large. On July 1, the absolute differences range from 1% to 10% higher when the shadow effect is included. For August 23, the range is from about −3% to +12% with much more variability than for July 1. With the instruments located in an area of maximum shadow, one might expect a large increase in radiation when this factor is allowed for; this is not the case, for two reasons. First, the sun is at a low angle during the extra hours of sunlight, and secondly, the upper basin points are not without shadow for the entire day; thus, they gain only perhaps 1–3 hours more sunshine than the micrometeorological site. On July 1, with the shadow effect included, the northwestern lobe with its southeasterly exposure gained only 1–3% more insolation; the western lobe had about a 5% increase; the southern lobe experienced a 5–6% increase; and the centre basin increased about 3%, except along the edge of the ice above Peter White Hut where the increase was about 10%. In late August the insolation variations with shadow were −3% to +3% for the northwestern basin, a 9%–12% increase for the western lobe, a 5%–10% increase in the southern lobe, and a 5% increase in the centre basin with an 8–9% increase by Peter White Hut.

The tongue of Peyto Glacier experiences the main losses because of shadow. During the high sun period the eastern side increased 5% with the inclusion of the shadow effect, but the western side of the tongue recorded a slight loss of 2%–3%. By late August the entire tongue experience from 0–3% decrease in the absolute daily total, when the areal shadow effect is considered, and a small region on the eastern side had a 16% drop because of its location close to mountain ridges. This gentle north-facing slope loses insolation because of the lower sun-path resulting in increased mountain shadow.

The two days illustrated here have a large direct shortwave component in the global radiation total. As shown in Table 1, however, there are several periods when

Figure 15. Upper Peyto sub-basins, view from southern lobe towards northwestern lobe (upper right) and centre basin (centre of photo).

Figure 16. View from base camp towards south. Snow-free, shadowed tongue is in foreground. Steep, north-facing slopes of the icefall and Mt. Rhondda are clearly visible.

the total is dominantly diffuse; under these conditions variations due to slope and aspect are minimal, even on the steep north vs. south facing slopes. Thus, a uniform global radiation input is characteristic over the entire glacier during heavy overcast, rainy periods.

THE RELATION BETWEEN ABLATION AND GLOBAL RADIATION

The final step in this analysis is an attempt to define any relation which may exist between the calculated areal distribution of global radiation and the measured ice melt over Peyto Glacier. The latter was defined by the total ice melt measured by the ablation stake network over the glacier (Fig. 17). The distribution of melt cannot be readily compared to that of radiation since there is a limited stake network over much of the upper basin, with much of the basin not having any stake coverage. It is observed that the transient snow line for Peyto Glacier follows the same NW-SE trend as the band of radiation noted earlier; also, the area where the highest radiation is received is observed to be the first ice-free area above the icefall, and its negative mass balance tends to be more than that of other parts of the upper basin. However, a light snowfall in this area, relative to other parts of the glacier, could be an important factor influencing the distribution.

Limited research has been directed towards the problem of radiation and the ablation of ice and snow, and the studies which have been carried out have been concerned largely with the energy transfers as determined at a single location. Hubley (1957) made a comprehensive study of the surface energy exchanges during the ablation season on Lemon Creek Glacier, Alaska, but he did not emphasize quantitative relationships between these processes and ablation. It is significant, however, that he found turbulent transfer of heat to be the most important factor in causing ablation on the Lemon Creek Glacier. Areal variations of this effect were not determined.

Mayo and Péwé (1963) followed up this research by studying the amount of heat exchange by radiation on glacial ice in central Alaska. Using net radiation and a single stake measurement they concluded that "in general, the amount of radiation received is less than the amount of heat required for ablation, and a rough correlation exists between the two" (p. 640).

Continuing to follow the energy balance approach, Federer (1968) studied radiation and snowmelt on a clearcut watershed in New Hampshire. Although studying the areal pattern, the study emphasized comparison of the snow-water content as predicted by the energy balance and the snow course measured values. Moderately good results were obtained in predicting snowmelt from the clearcut mountainous watershed; their particular problem was determining the effect of the slash on snowmelt.

The problem at hand, however, is to look at the problem spatially. Rouse and Wilson (1969) mapped the variation of global radiation over Mt . St. Hilaire, but despite concern with snow distribution and melt, no quantitative analysis of the relation between these and radiation was attempted, other than a statement that the south slope was snow-free a full three weeks before the north slope.

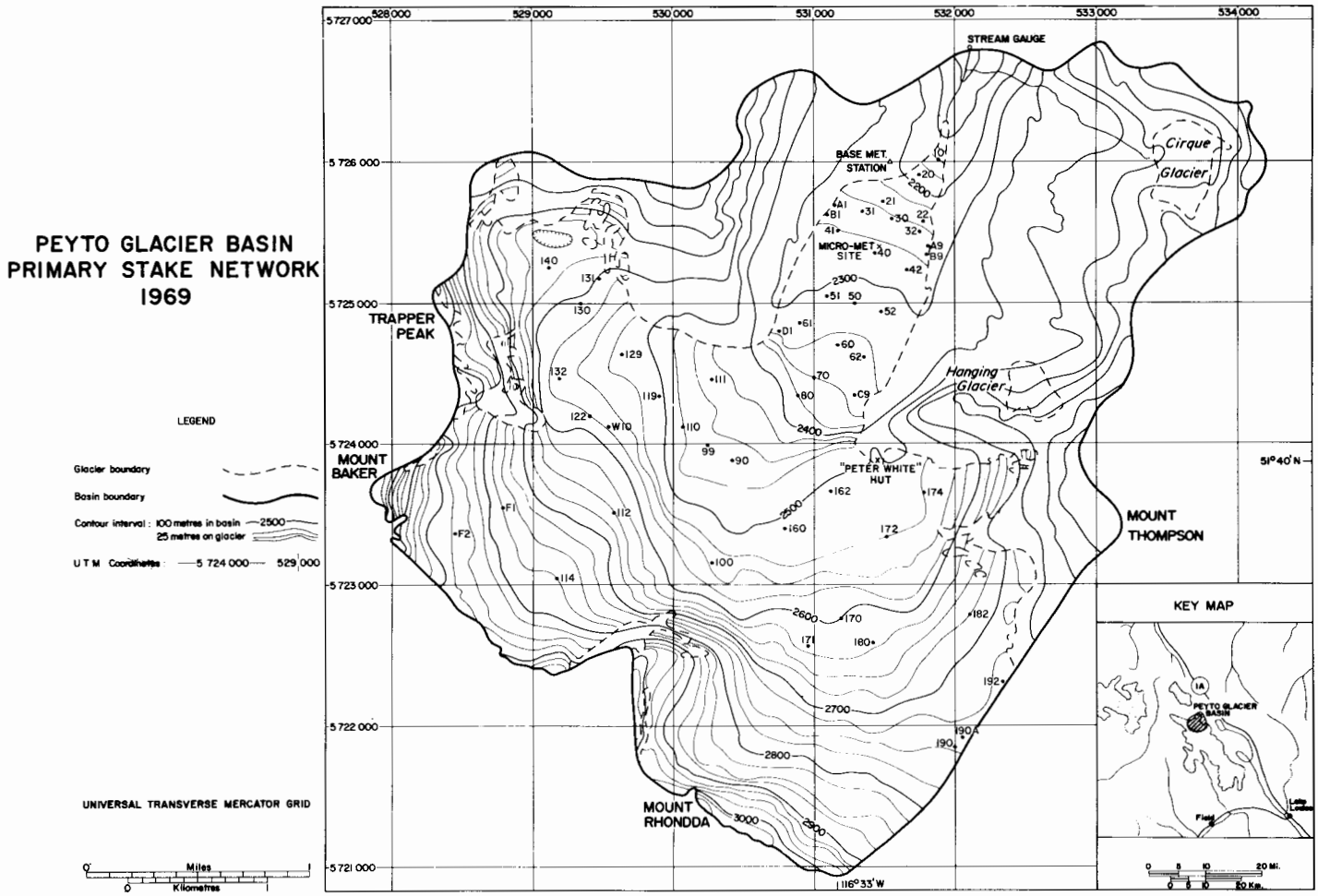

Figure 17. Peyto Glacier Basin, primary stake network, 1969.

The present study looks at the radiation ablation problem from this spatial context. Daily global radiation distributions for the period August 16 – September 1 were calculated based on measured diffuse and direct radiation at the micrometeorological site. Complete runs were made for both the "shadow" and "no-shadow" effect over the glacier.

Thirty-eight stakes provided ablation data for two sample periods. The first was for August 15 – August 31; 23 stakes were used and covered the tongue of the glacier. The other period was August 15 – September 1, and 15 stakes from the upper basins were used in the analysis. The total amount of ice lowering during these periods was used as the measured ablation; density of the ice was assumed constant.

To obtain comparable global radiation totals for each stake, spatial averages based on the 200–m grid were used to calculate the daily global radiation applicable to the selected stakes. Totals were then obtained for the periods under study. The results obtained are listed in Table 2; there are two radiation totals–one excluding the shadow effect, the other including the influence. The percentage change in the radiation total because of the inclusion of the shadow effect is also presented; the changes are neither highly variable nor great. For the tongue of the glacier (Sample 1) there was basically a reduction in radiation received, with a mean decrease of –0.6%. For the area above the icefall, there is an increase in radiation received, but the changes are even with a mean increase of +1.8%. The small change due to shadow effects is similar to that obtained from the study of the distribution over Peyto Glacier. The small percentage changes, however, are almost negligible, and in terms of the spatial pattern it could be omitted without any loss of information.

Using these two samples, a simple correlation analysis was carried out. The results are shown in Table 3.

The above results, which indicate no relation between the two variables, may seem surprising but considering that global radiation is only one part of the radiation balance, they should not seem so. The inclusion of the shadow

Table 2. Summary of global radiation and ablation analysis

a) August 15 – August 31, 1969: Sample 1

Stake No.	Ablation (cm)	Global Radiation Total (no shadow) (1y)	Global Radiation Total (shadow effect included) (1y)	% Change
80	25	5947.8	5946.8	−0.0
70	66	6011.8	6039.6	+0.5
62	42	6196.6	5937.2	−4.2
61	40	5815.9	5933.2	+2.0
60	34	5935.9	6018.9	+1.4
52	47	6098.1	6051.4	−0.8
51	33	6083.1	6006.2	−1.3
50	38	6085.0	6044.3	−0.7
42	50	6043.4	6028.3	−0.2
41	33	6086.8	6034.1	−0.9
40	56	6037.8	6039.9	+0.0
32	47	5768.2	5841.1	+1.3
31	32	5962.3	5911.6	−0.9
30	61	5881.8	5845.4	−0.6
22	52	5562.4	5530.9	−0.6
21	64	5812.5	5733.9	−1.4
20	45	5711.6	5622.9	−1.6
10	33	5772.1	5668.3	−1.8
B9	59	5998.1	5963.6	−0.6
A9	49	5976.9	5932.0	−0.8
A1	65	6037.8	5972.0	−1.1
D1	72	5843.2	5896.1	+0.9
C9	45	6206.3	6007.4	−3.2
				Mean = −0.6

b) August 15 – September 1, 1969: Sample 2

Stake No.	Ablation (cm)	Global Radiation Total (no shadow) (1y)	Global Radiation Total (shadow effect included) (1y)	% Change
111	46	6458.0	6598.1	+2.2
99	64	6659.3	6774.8	+1.7
90	33	6557.2	6639.8	+1.3
180	28	6460.0	6631.0	+2.6
174	42	6659.3	6795.6	+2.0
171	36	6210.8	6393.3	+2.9
170	43	6436.0	6591.7	+2.4
162	22	6426.8	6520.6	+1.5
160	37	6500.0	6618.6	+1.8
132	36	6519.6	6626.3	+1.6
131	35	7126.1	7107.1	−0.2
130	34	7006.6	7075.2	+1.0
129	34	6870.3	7020.6	+2.2
122	41	6247.0	6352.1	+1.7
110	38	6620.2	6762.8	+2.2
				Mean = +1.8

effect causes a negligible change, but the shift is in the supposedly right direction. Why then does there appear to be no relationship between global radiation and ablation over the glacier?

Table 3. Correlation of ablation and global radiation

	Global Radiation (no shadow effect)	Global Radiation (shadow effect included)
Sample 1	−0.14	−0.08
Sample 2	−0.00	+0.02

Garstka et al. (1958) found little relation in their multiple regression analysis of snowmelt and meteorological parameters. They used solar radiation measured at one location as an independent variable, but in the analysis its regression coefficient tended to have a negative sign. This was not expected since the sun is the ultimate source of all energy used in snow melting. At the time they attributed the result to high intercorrelation with another independent variable, degree-days above 32°F. Naturally, this is possible but if the partial correlation coefficients had been available, it would have been possible to see the actual relation.

More recent work by Megahan et al., (1967), however, on the relation between radiation and snowmelt at a point gives support to the present study's results. In a simple regression analysis they found incoming shortwave radiation could explain only 3% of the variation in melt at a point, while net all-wave radiation could explain 91% of the variation. The key here is albedo and the long-wave radiation exchange between snow and air. Their project was to investigate the acceleration of snowmelt by decreasing the albedo; at this time they found net all-wave to be the more suitable predictor. Physically this is reasonable, but the application of this to a basin for the purposes of studying spatial variation is the problem that will need further research.

The study of the global radiation over Peyto Glacier is the necessary first step in the study of radiation and ablation of snow and ice. Shadow, which has the greatest direct effect on global radiation distribution, has been seen to have negligible effect on the spatial pattern of radiation income or on the relation to ablation. Other factors in the radiation balance must be considered.

Albedo is a crucial parameter as it determines the amount of shortwave insolation which will actually be absorbed. The problem is to determine the spatial variation of albedo over the glacier. The surface texture of Peyto Glacier varies greatly – the matrix composition of ice and glacial debris is very variable and the amount of water over the surface changes. In short, the physical characteristics of the glacier surface are quite changeable, with marked

differences above and below the icefall. The differences between a snow or ice cover also are important in influencing the rate of melt. Hubley (1957) showed that because of albedo effects, the amount of solar radiation absorbed by a bare ice surface in early September may be greater than the absorption by a snow-covered glacier surface in early June. In the present study, all these physical changes would have a critical role in the disposition of incoming insolation and therefore in the amount of energy available for the melt process. In addition, Hubley (1955, 1957) found albedo to vary with the time of day, cloudiness, latitude, elevation above sea level, season, and the aspect and gradient of the surface slope. To combine these factors into a spatial distribution for Peyto Glacier will be a formidable task. A single albedo measurement is definitely not applicable to the entire surface.

The other important radiation term is the net long-wave flux affecting the melt process. This may be quite important on overcast days when the net flux may be positive at the surface. On clear days, long-wave emission from the land may influence melt at the edge of the glacier, but it will not likely influence melt over the central upper basins.

Other considerations should include estimation of the latent heat flux during the ablation period, and consequently the loss or gain of energy from the system, and it would be useful to have an estimate of the contribution to melt by the turbulent transfer of heat from summer storms. This may be significant over Peyto Glacier, as it was in Alaska.

It is evident that much more information is needed, not so much on daily variations at a point – this has been investigated in the recent past – but on spatial variation over a glacier. This will not be an easy task, as it will be difficult to measure simple parameters which can be adequately adjusted for spatial variations.

CONCLUSIONS AND RECOMMENDATIONS

The present study is the initial research into the distribution of radiation over Peyto Glacier and/or Peyto Basin. From this work on global radiation it is evident that there is a significant difference in the received solar radiation depending on a point's slope and azimuth, and in many cases on its shadow conditions. However, these differences alone do not dictate any statistically meaningful relationship between global radiation and ablation. Previous study found no relationship for a single horizontal site; this study found no relationship between the two in a spatial context, allowing for aspect, gradient and shadow.

Consideration of the effect of shadow on the distribution of global radiation and the absolute variation of radiation involves exhaustive calculations and considerable time. To study only the distribution of radiation it is debatable whether the inclusion of the shadow effect is necessary. During the lower sun periods changes due to shadow are increased, and probably later in the season they will be more pronounced. However, if the hour angles are not available over the glacier for the selected day and consequently the shadow effect cannot be included, a reliable distribution pattern for global radiation can be obtained without them. Once they have been worked out for any day, though, the adjusted hour angles are applicable in any year. In such a situation the shadow should be included.

The main recommendation, from an analytical point of view, is in reference to the location of the radiation instruments. It is realized that the present site was located on the ice near the camp so that detailed measurements of several meteorological variables could be easily made, but, since the site was on the ice, it needed constant levelling. In addition, this is an area of maximum shadow, and radiation is recorded for only 75% of the total possible number of hours of sunshine. Because of the mountain location it is virtually impossible to locate the instrument in a position where it will record all incoming radiation, but a value of 90% should not be impossible to attain.

If continuous measurements of direct and diffuse shortwave radiation are to be collected in the future, the instruments should be placed in a more representative location, preferably in the centre basin. If they were installed over ice there would be the problem of constant daily re-levelling; it is suggested that radiation instruments and other meteorological instruments (e.g., recording rain gauge, Stevenson Screen, anemometer) be installed on the rock outcrop above stake 90. Here shadow problems would not be serious and the point would be more representative of the upper reaches of the glacier which make up 85% of the total glacier area.

If the instrument were positioned here it could not be visited daily; this means that a different type of shade ring which required adjusting only every three or four days, or longer, would be necessary. It is understood that a shading ring which fits the Kipp instrument and which is calibrated to provide a correction for the diffuse radiation intercepted by the ring, could be made available by the Ministry of Transport (now Atmospheric Environment Service Dept. of the Environment). Shading rings for the Kipp instrument have been made by M.O.T. for their own use; investigation of the possibility of obtaining one is highly recommended.

In summary it is clear that global radiation values adjusted for azimuth, gradient, and shadow are much more meaningful on a basin-wide scale than a single value recorded at a non-representative site. It remains to develop methods of estimating albedo and long-wave variations over both time and space. In short, is it possible to correct net all-wave values for these spatial and temporal variations as has been done in this study for global radiation? At this stage, the ablation and radiation relationship should be much clearer.

ACKNOWLEDGMENTS

The advice of Atsumu Ohmura (McGill University) in reference to the operation of the computer program is gratefully acknowledged. Thanks are extended to L. Derikx, T. Bellaar-Spruyt and S. Monroe for their advice and help in the field. Finally, the constant encouragement and advice from Dr. A. Stanley and Dr. O.H. Lϕken has been of great benefit.

REFERENCES

Bolsenga, S.J. 1964. Daily Sums of Global Radiation for Cloudless Skies. *CRREL Research Report* 160, Hanover, New Hampshire, 124 p.

Canada, Department of Transport, Meteorological Branch. *Monthly Radiation Summary, December 1969.*

Federer C.A. 1968. Radiation and Snowmelt on a Clearcut Watershed. *Proceedings, Eastern Snow Conference, 1968,* pp. 28-42.

Garnier, B.J. 1968. Estimating the Topographic Variation of Direct Solar Radiation; A Contribution to Geographical Microclimatology. *Canadian Geographer*, XII, No. 4, pp. 241-248.

Garnier, B.J. and A. Ohmura. 1968. A Method of Calculating Direct Shortwave Radiation Income of Slopes. *J. of Applied Meteorology,* vol. 7 (Oct.), pp. 796-800.

Garnier, B.J. and A. Ohmura, 1970. The Evaluation of Surface Variations in Solar Radiation Income, *Solar Energy,* vol. 13, pp. 21-34.

Garstka, W.U., L.D. Love, B.C. Goodell, and F.A. Bertle. 1958. *Factors Affecting Snowmelt and Streamflow.* U.S. Dept. of the Interior, Bureau of Reclamation and U.S.D.A. Forest Service, 189 p.

Hubley, R.C. 1955. Measurements of Diurnal Variations in Snow Albedo on Lemon Creek Glacier, Alaska. *Trans. A.G.U.*, v. 38, pp. 68-95.

Hubley, R.C. 1957. Analysis of Surface Energy During the Ablation Season on Lemon Creek Glacier, Alaska. *Trans. A.G.U.,* v. 38, pp. 68-95.

Kondrat'yev, K. Ya. 1965. *Radiative Heat Exchange in the Atmosphere.* New York: Pergamon Press, 411 p.

List, R.J. 1966. *Smithsonian Meteorological Tables,* 6th revised edition Washington: Smithsonian Institution, 527 p.

Mayo, L. and T.L. Péwé. 1963. Ablation and Net Radiation, Gulkana Glacier, Alaska. In *Ice and Snow* (ed. W.D. Kingery). M.I.T. Press, pp. 633-643.

Megahan, W.F., J.R. Meiman, and B.C. Goodell. 1967. Net Allwave Radiation as an Index of Natural Snowmelt and Snowmelt Accelerated with Albedo Reducing Materials. In *International Hydrology Symposium,* Fort Collins, v. 1, pp. 149-156.

Ohmura, A. 1968. The Computation of Direct Insolation on a Slope. *Climatological Bulletin* (McGill University), No. 3, January, pp. 42-53.

Rouse, W.R. and R.G. Wlson. 1969. Time and Space Variations in the Radiant Energy Fluxes over Sloping Forested Terrain and their Influence on Seasonal Heat and Water Balances at a Middle Latitude Site. *Geogr. Annaler,* Ser. A, v. 51, No. 3, pp. 160-175.

Sedgwick, K. 1966. *Geomorphology and Mass Budget of Peyto Glacier, Alberta,* Unpublished M.A. Thesis, McMaster University, 165 p.

Sellers, W.D. 1965. *Physical Climatology.* Chicago: University of Chicago Press, 272 p.

U.S. Navy Department, Hydrographic Office, 1940. *Tables of Computed Altitude and Azimuth, Latitudes 50° to 59° Inclusive.* Washington, U.S. Printing Office, pp. 28-79.

APPENDIX

Formulae for determining radiation totals at selected stakes.

The following formulae apply to the matrix output of radiation totals. Numbers are the vertical coordinate; letters are the horizontal coordinate.

Stake No.	Formula
90	13M
99	2/3 12 L + 1/3 12M
110	$\frac{11K + 11L + 12K}{3}$
111	$\frac{10L + 10M}{2}$
119	$\frac{10J + 10K + 11J + 11K}{4}$
160	43A
100	$\frac{16L + 16M + 17L + 17M}{4}$
122	11H
129	9I
132	10G
130	7H
131	2/3 6H + 1/3 6I
140	2/3 6G + 1/3 6F
162	2/3 42B + 1/3 42C
172	$\frac{43E + 44E + 44D}{3}$
174	42F
171	1/3 47B + 2/3 48B
170	$\frac{46C + 47C}{2}$
180	$\frac{47D + 48D}{2}$
182	$\frac{46G + 46H + 47H}{3}$
10	30F
20	$\frac{30F + 31F}{2}$

Stake No.	Formula
21	$\frac{31D + 31E}{2}$
22	32F
30	32E
31	32D
32	$\frac{32F + 33F}{2}$
40	33D
41	33C
42	$\frac{34F + 34E}{2}$
50	$\frac{35C + 35D}{2}$
51	$\frac{35B + 35C}{2}$
52	$\frac{35D + 35E + 36D}{3}$
60	$\frac{36C + 37C}{2}$
61	$\frac{36A + 36B}{2}$
62	37D
70	1/3 37B + 2/3 38B
80	$\frac{38B + 39B}{2}$
A9	33F
B9	$\frac{33F + 34F}{2}$
A1	32C
D1	36A
C9	1/3 38C + 2/3 38D

=

GB
707
C335
No.22

Goodison, Barry

The distribution of global radiation over Peyto Glacier, Alberta.